Lock-and-Key and Shape-Memory Effects in an Unconventional Synthetic Path to Magnesium-Organic Frameworks

Huajun Yang, Thuong Xinh Trieu, Xiang Zhao, Yanxiang Wang, Yong Wang, Pingyun Feng, Xianhui Bu**

Abstract: *From Mg-containing chlorophyll in CO_2 fixation to the Mg-form of MOF-74 in high-capacity CO_2 capture, the special relationship between Mg coordination compounds and CO_2 has fascinated generations of researchers. We report here a new magnesium MOF (**CPM-107**) with special interaction with CO_2. CPM-107 contains Mg_2-acetate chains crosslinked into a 3D net by terephthalate. It features an anionic framework encapsulating ordered extra-framework cations and solvent molecules. The desolvated form is closed and unresponsive to common gasses such as N_2, H_2, and CH_4. Yet, with CO_2 at 195K, it abruptly opens and turns into a rigid porous form that is irreversible via desorption. Once opened by CO_2, CPM-107 remains in the stable porous state accessible to additional gas types over multiple cycles or CO_2 itself at higher temperatures. The porous phase can be re-locked to return to the initial closed phase via re-solvation and desolvation. Such peculiar properties of CPM-107 are apparently linked to a convergence of factors related to both framework and extra-framework features. The unusual CO_2 effect is currently the only available path to porous CPM-107 which exhibits* an *efficient C_2H_2/CO_2 separation property.*

Metal-organic frameworks (MOFs) or porous coordination polymers (PCPs) have some unique properties not usually found in zeolites and other porous materials.[1] One is the dynamic feature of so-called third-generation PCPs (also known as soft or flexible MOFs).[2] These MOFs can respond to a range of stimuli (especially guest adsorption/desorption), which can be exploited for applications including gas storage/separations, drug release, catalysis, and sensing.[3] However, it has been reported that fewer than 1% MOFs are known for such stimuli-responsive properties.[4]

In some flexible MOFs, stepped gas-adsorption isotherms with gate-opening behavior have been observed, and the process typically involves a closed-pore or narrow-pore structure that expands to an open-pore structure after reaching a certain threshold of gas pressure.[5] Such gate-opening behavior is related to the balance between the framework flexibility and the gas-framework interaction and varies for different gas-framework pairs.[6] An extreme case would be the gate opening under a specific condition and by a specific gas. So far, few examples of such specificity are known,[7] although some flexible MOFs did show different gate-opening pressure for different gases.[8]

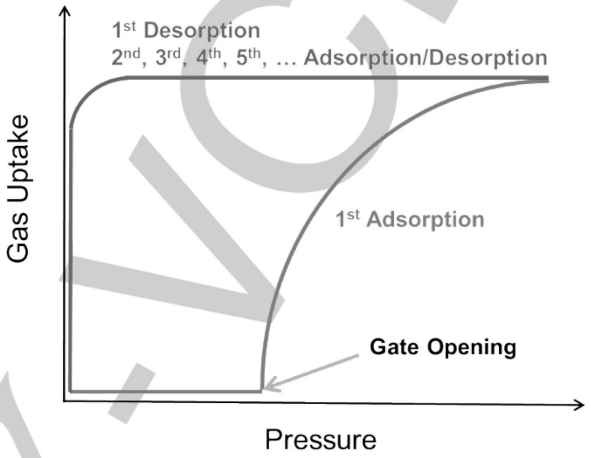

Scheme 1. Flexible-to-rigid transformation in shape-memory metal-organic frameworks with gate opening.

It has also been observed that most of the flexible MOFs have reversible structural transformation where the initial state is fully or mostly restored through desorption, albeit with the hysteresis.[9] Interestingly, Kitagawa et al. demonstrated that one type of flexible MOFs could transform into rigid phase by reduction of crystal size, leading to so-called shape-memory MOFs (Scheme 1).[10] The open-dried phase is kinetically stable over further gas adsorption experiments and can revert to the closed one via heat and vacuum, similar to the general shape-memory effect observed in polymers, metals, and so on.[11] Recently, Zaworotko et al. reported two shape-memory MOFs without crystal downsizing.[12] These rare examples of shape-memory MOFs are based on paddlewheel dimers with the pcu topology (Table S2).

In this work, we report an unusual MOF (CPM-107) built from $[Mg_2Ac]^{3+}$ chains and without Mg-solvent bonds (i.e., no open metal sites in the desolvated form).[13] The desolvated phase of CPM-107 (hereafter **CPM-107cl**) selectively responds to CO_2 over CH_4, N_2, and H_2 and transforms into an open dried phase (**CPM-107op**) with a typical gate-opening isotherm. The open phase is sustainable over multiple adsorption/desorption cycles. The pore in the open phase, enabled by CO_2 only, can be accessed with CH_4, N_2, and H_2 (lock-and-key effect). We could only re-generate CPM-107cl phase by repeating the activation procedure, that is, soaking in CH_2Cl_2 and then desolvating under vacuum (shape-memory effect).

[*] Dr. H. Yang, T. X. Trieu, and Prof. X. Bu
Department of Chemistry and Biochemistry, California State University, Long Beach, California 90840 (United States)
E-mail: xianhui.bu@csulb.edu
Dr. X. Zhao, Y. Wang, Dr. Y. Wang, and Prof. P. Feng
Department of Chemistry, University of California
Riverside, California 92521 (United States)
E-mail: pingyun.feng@ucr.edu

Supporting information and the ORCID identification number(s) for the author(s) of this article can be found under:

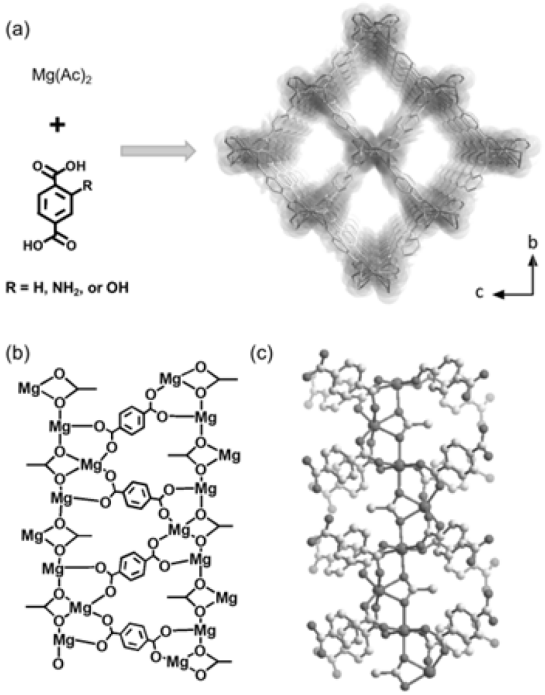

Figure 1. (a) The building scheme of **CPM-107**. (b) Connection between two adjacent Mg_2-acetate chains. (c) ball-and-stick diagram of the Mg_2-acetate chain.

Reaction of $Mg(Ac)_2$, H_2BDC, and acetic acid in DMA and water afforded colorless rod-like crystals (denoted as **CPM-107as**, Figure 1). The phase purity is confirmed by PXRD (Figure S1). Using 2-NH_2-H_2BDC and 2-OH-H_2BDC ligands under similar conditions led to **CPM-107NH$_2$** and **CPM-107OH** (Table S1). CPM-107as crystallizes in a chiral orthorhombic space group $P2_12_12_1$. Given that it has two types of crosslinking ligands and two types of extra-framework species, it has a long formula $[Mg_2(BDC)_2(Ac)][(CH_3)_2NH_2](DMA)_2$. Its asymmetric unit contains two crystallographically independent Mg^{2+} cations, two BDC^{2-} anions, one acetate anion, one protonated dimethylamine, together with two independent DMA solvent molecules, all of which can be located (Figure S2). Both Mg sites are octahedrally coordinated to six oxygen atoms but with different coordination configuration (Figure S3). It is worth noting that all six coordination sites of Mg are used for the formation of the framework and therefore CPM-107 has no solvent binding sites. This is uncommon considering that Mg-MOFs grown from polar solvents often contain Mg-solvent bonds.

CPM-107 has a rod-packing architecture with sql pattern based on Mg_2-acetate chain. Each acetate anion uses its two oxygen atoms to bridge Mg1 into an infinite $[Mg\text{-}CH_3COO]^+$ chain. Both of these two oxygen sites from the same acetate anion also chelate to the Mg2 site. As such, Mg2 can be considered as being appended to the Mg1-CH_3COO chain and the chain thus has the overall composition of $[Mg_2(CH_3COO)]^{3+}$. These chains are oriented along the crystallographic *a* axis, leading to 1D channels (Figure 1).

The gas adsorption was studied for N_2 (77 K), H_2 (77 K), CH_4 (195 K, 273 K, and 298 K), and CO_2 (195 K, 232 K, 273 K, and 298 K). For activation, all the samples were subject to a solvent exchange in CH_2Cl_2 for 3 days and subsequently exposed to dynamic vacuum at 60 °C. IR spectra, together with NMR spectra from a digested sample showed that the solvent exchange was complete (Figure S5-6).

In comparison with the commonly observed gate opening, CPM-107 shows an unusual gate-opening behavior, because its pore could not be opened by common gases except CO_2 and the opened phase could not transform back to the closed phase upon desorption. Specifically, it showed negligible uptake for N_2 at 77 K. The same was true in H_2 adsorption at 77 K and CH_4 adsorption at 195 K, and CO_2 adsorption at 232 K and 273 K. When it came to CO_2 adsorption at 195 K, however, a different, yet interesting behavior was discovered. In the adsorption isotherm (Figure 2a), there was no appreciable adsorption up to 380 Torr and then a steep uptake increase was observed with the increase in the pressure, leading to a saturation uptake as high as 206 cm^3/g. Such adsorption feature is indicative of a gate-opening effect, corresponding to the structural transformation from a closed-pore framework (CPM-107cl) to an open-pore framework (CPM-107op). The desorption trace was also found to not follow the adsorption branch, giving a very large hysteresis. A high uptake was maintained even at a very low pressure. Note that in general, the desorption trace eventually followed the adsorption one with very small uptake at low pressure for most flexible MOFs. It indicated that the CPM-107op was stable upon desorption like rigid frameworks.

The occurrence of three distinct phases (CPM-107as, CPM-107cl, and CPM-107op) was verified by PXRD (Figure S7). The first peak in PXRD pattern of CPM-107cl exhibited a shift to the higher angle (around 8.8 degree) by about 1 degree compared with that of CPM-107as and CPM-107op, which is likely due to the lattice shrinkage.[14] Given the relatively small pore size in CPM-107, together with the pore-blocking role by extra-framework cations, even a minor structural change can dramatically impact the accessibility of the pore space.

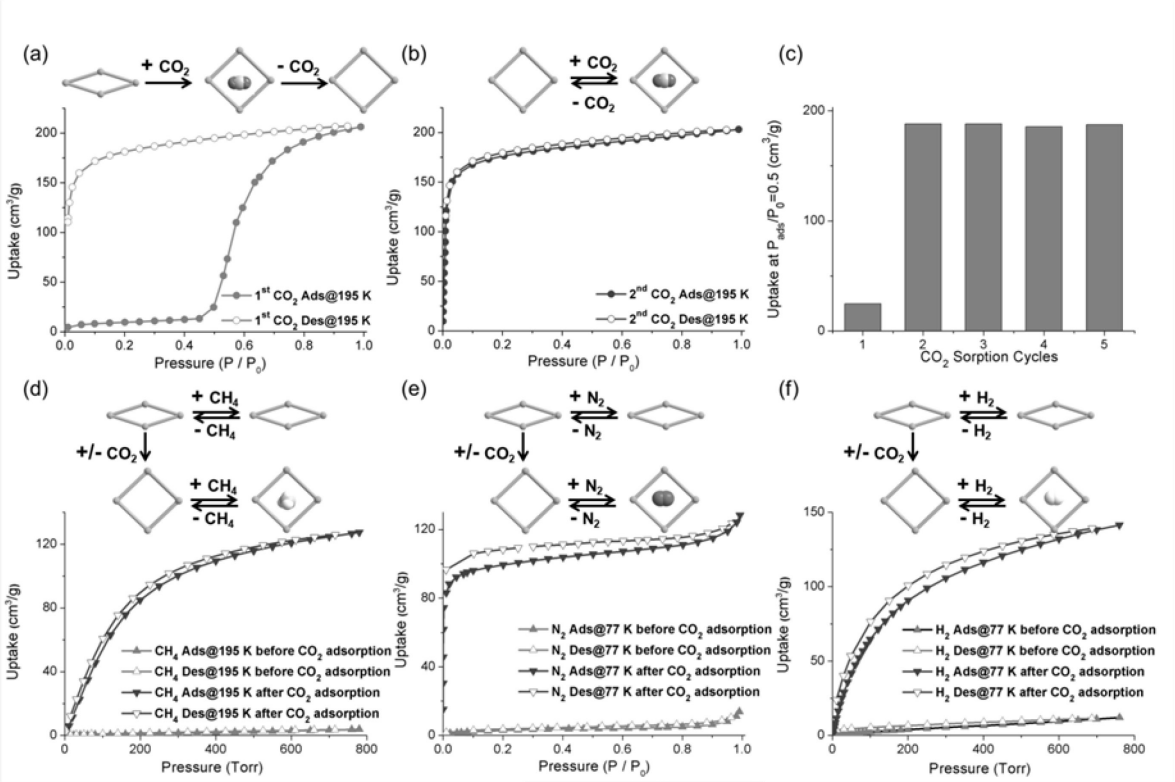

Figure 2. (a) The first cycle of CO_2 adsorption/desorption isotherms of CPM-107 at 195 K. (b) The second cycle of CO_2 adsorption/desorption isotherms of CPM-107 at 195 K. (c) Comparison of CO_2 uptake at P_{ads}/P_0=0.5 of the first five cycles at 195 K. (d) CH_4 adsorption/desorption isotherms of CPM-107 at 195 K before and after CO_2 adsorption. (e) N_2 adsorption/desorption isotherms at 77 K of CPM-107 before and after CO_2 adsorption. (f) H_2 adsorption/desorption isotherms at 77 K of CPM-107 before and after CO_2 adsorption.

CPM-107op was stable and could be accessed by other common gases (N_2, H_2, and CH_4) which show negligible adsorption in the closed phase. A typical type-I isotherm was observed for the second cycle of CO_2 adsorption at 195 K, which coincides with the desorption trace of the first cycle (Figure 2b). Such adsorption isotherm could be repeated (three additional cycles of CO_2 sorption experiments at 195 K were performed) (Figure S8&2c). After the pore opening at 195 K by CO_2, CO_2 adsorption at 273 K and 298 K also showed type-I isotherms with the saturation uptake of 67 and 35 cm^3/g (Figure S9). Besides, after CO_2 adsorption at 195 K, pronounced adsorption uptake with type-I isotherms have also been found in CH_4 adsorption at 195 K, N_2 and H_2 adsorption at 77 K (Figure 2d-f). The small open hysteresis observed in CH_4, N_2 and H_2 isotherms is probably due to the narrow pore of CPM-107op.[15]

Based on N_2 adsorption at 77 K, the Brunauer-Emmett-Teller surface area and Langmuir surface area of CPM-107op were determined to be 319 and 444 m^2/g, respectively, with t-plot micropore volume of 0.146 cm^3/g. In comparison, using the crystal data of CPM-107as (DMA solvents are deleted manually), GCMC simulation showed that the simulated saturated uptake at 77 K is 235 cm^3/g, almost twice the measured value for CPM-107op (Figure S10). The theoretical BET surface area is estimated as 1037 m^2/g. These results indicated that the open form does not correspond to the as-synthesized framework, which is also consistent with the PXRD patterns (Figure S6).

This type of flexible-to-rigid transformation was rare, and has been observed in known shape-memory MOFs and one flexible indium MOF.[10, 12, 16] Notably, in previously known shape-memory MOFs, the 'memory' phase could be recovered from the open phase upon another stimuli including heat, vacuum, or solvent soaking. In this work, we were unable to use heat and vacuum to return CPM-107op back to CPM-107cl (Figure S12). Inspired by the activation process which induced the structural transformation from CPM-107as to CPM-107cl, we reasoned that CPM-107cl might be regenerated again via repeating the activation process. Indeed, after immersing CPM-107op in CH_2Cl_2 for about eight hours, the subsequent desolvation process led to the reverse structural transformation from CPM-107op back to CPM-107cl, as verified by PXRD patterns (Figure S13). This is probably due to the stronger interaction of CH_2Cl_2 with the framework (compared to gas molecules).[17] Further CO_2 adsorption experiments at 195 K could also reproduce the gate-opening isotherm and flexible-to-rigid transformation (Figure S14).

We also tried to realize the transformation from CPM-107cl to CPM-107as via soaking CPM-107cl in DMA which is the solvent trapped in CPM-107as. However, PXRD did not show the

occurrence of CPM-107as (Figure S15). A comprehensive scheme for all the structural transformations was proposed in Figure S16.

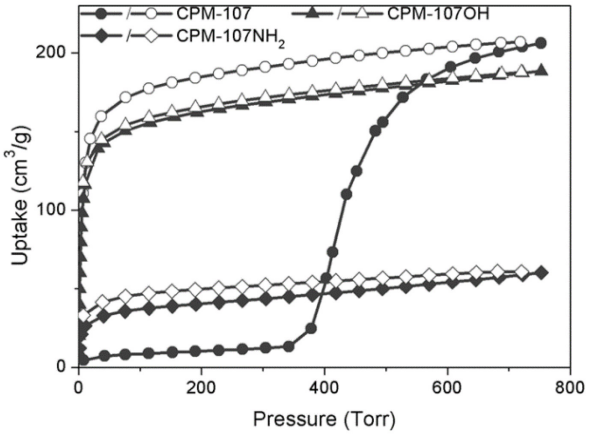

Figure 3. The first cycle of CO_2 adsorption/desorption isotherms of CPM-107, CPM-107OH, and CPM-107NH_2 at 195 K.

Both CPM-107NH_2 and CPM-107OH were found to have the adsorption behavior of rigid MOFs, as shown by the type-I CO_2 adsorption isotherm at 195 K (Figure 3). This means that, unlike CPM-107as, CPM-107NH_2 and CPM-107OH are not transformed into a closed-pore form during the activation process. PXRD patterns showed that their structures remained intact after gas adsorption (Figure S17-18).

While we were unable to perform single-crystal structure analysis on CPM-107cl and CPM-107op due to poor crystal quality, it might be possible to gain some understanding from the comparison with other chain-type structures.[18] The structural transformations in CPM-107 may be related to the ligand hinge motion, but it was probably more complicated since the BDC ligand was distorted in bridging the adjacent chains in CPM-107. Such coordination distortion could also be observed in a Co(bdp) structure (bdp^{2-} = 1,4-benzenedipyrazolate) (Figure S19).[19] It was notable that CPM-107 has an anionic framework, meaning that all the framework-guest interactions were mediated by the cationic $[NH_2(CH_3)_2]^+$ which may also contribute to the rigidity of CPM-107op.[20] Beside, due to the delicate flexibility of CPM-107, it easily transformed into rigid ones through using ligands with substituent group (CPM-107NH_2 and CPM-107OH) in which the hinge motion may be restricted due to the larger steric hindrance and intramolecular H-bonding (Figure S20).

CPM-107op exhibited moderate CO_2 affinity with an uptake of 37 cm^3/g at 298 K. The isosteric heat of adsorption (Q_{st}) near the zero coverage was calculated to be 24 kJ $mmol^{-1}$. Note that CPM-107 has no open metal sites. The potential application of CPM-107op for C_2H_2/CO_2 separation was then studied. Separation of CO_2 from C_2H_2 is important in industrial applications but is also challenging due to their similar size and physicochemical properties.[21] It is intriguing to find that CPM-107op can take up 136.7 cm^3/g and 97.5 cm^3/g of C_2H_2 at 273 K and 298 K (Figure S21), respectively. The uptake capacity at 298 K is higher than some benchmark C_2H_2/CO_2-separation materials such as UTSA-300 (67 cm^3/g) and HOF-3 (47 cm^3/g).[22] The isosteric heat for C_2H_2 adsorption is also calculated to be in the range of 32-37 kJ $mmol^{-1}$, apparently larger than that of CO_2 (Figure 4). To evaluate the potential separation capability of CPM-107op, the ideal adsorbed solution theory (IAST) is applied to calculate the selectivity of C_2H_2/CO_2 in the equal mixture at 298 K (Figure S22-23). The result indicated that CPM-107op has the selectivity as high as 5.7 at 298 K and 1 atm, higher than FJU-90 (Table S3).[23] The combination of high C_2H_2 uptake capacity and the high C_2H_2/CO_2 selectivity shows that CPM-107op is among the best materials for C_2H_2/CO_2 separation. The CO_2 effect actually provides a unique path toward this high-performance material.

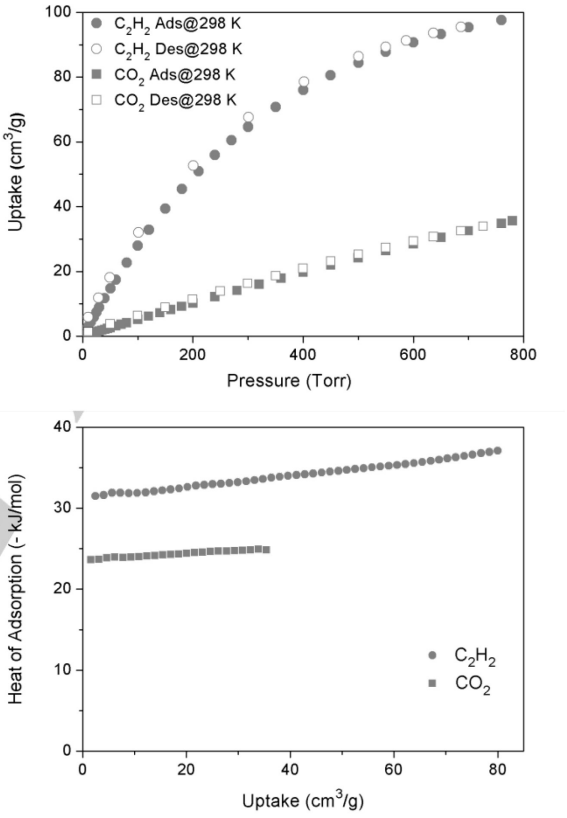

Figure 4. C_2H_2 and CO_2 adsorption isotherms of CPM-107op at 298 K (top) and their corresponding heat of adsorption (bottom).

In conclusion, while various types of flexible MOFs have been reported, we demonstrated here an extraordinary example in terms of the unique combination of lock-and-key effect (i.e., guest-selective yet irreversible gate opening) and shape-memory effect. The presence of a gas adsorption step in a synthetic path to a permanently porous material from a non-porous phase is an inspiring success in our continual search for new porous materials. The discovery of shape-memory phenomenon in a structural type different from the previously known pcu type suggests the possible existence of such shape-memory effect in a broader range of porous materials and may

also help improve our understanding of shape-memory effect in crystalline porous materials in general.

Acknowledgements

We thank the support by NSF-DMR, under award NO. 1708850 (X.B.) and CSULB RSCA award (X.B.).

Conflict of interest

The authors declare no conflict of interest.

Keywords: lock-and-key• shape-memory• magnesium metal-organic framework • CO_2 adsorption

[1] a) S. Kitagawa; R. Kitaura, S. i. Noro. *Angew. Chem. Int. Ed.,* **2004**, *43*, 2334-2375; b) H. Furukawa; K. E. Cordova; M. O'Keeffe, O. M. Yaghi. *Science,* **2013**, *341*, 1230444; c) G. Férey. *Chem. Soc. Rev.,* **2008**, *37*, 191-214.

[2] a) S. Horike; S. Shimomura, S. Kitagawa. *Nat. Chem.,* **2009**, *1*, 695; b) G. Férey, C. Serre. *Chem. Soc. Rev.,* **2009**, *38*, 1380-1399; c) A. Schneemann; V. Bon; I. Schwedler; I. Senkovska; S. Kaskel, R. A. Fischer. *Chem. Soc. Rev.,* **2014**, *43*, 6062-6096; d) T. D. Bennett; A. K. Cheetham; A. H. Fuchs, F.-X. Coudert. *Nat. Chem.,* **2017**, *9*, 11; e) Z. Chang; D. H. Yang; J. Xu; T. L. Hu, X. H. Bu. *Adv. Mater.,* **2015**, *27*, 5432-5441.

[3] a) C. Serre; F. Millange; C. Thouvenot; M. Nogues; G. Marsolier; D. Louër, G. Férey. *J. Am. Chem. Soc.,* **2002**, *124*, 13519-13526; b) C. Serre; C. Mellot-Draznieks; S. Surblé; N. Audebrand; Y. Filinchuk, G. Férey. *Science,* **2007**, *315*, 1828-1831; c) J. A. Mason; J. Oktawiec; M. K. Taylor; M. R. Hudson; J. Rodriguez; J. E. Bachman; M. I. Gonzalez; A. Cervellino; A. Guagliardi; C. M. Brown; P. L. Llewellyn; N. Masciocchi, J. R. Long. *Nature,* **2015**, *527*, 357; d) A. J. Fletcher; K. M. Thomas, M. J. Rosseinsky. *J. Solid State Chem.,* **2005**, *178*, 2491-2510; e) L. Li; R.-B. Lin; R. Krishna; X. Wang; B. Li; H. Wu; J. Li; W. Zhou, B. Chen. *J. Am. Chem. Soc.,* **2017**, *139*, 7733-7736; f) J.-P. Zhang, X.-M. Chen. *J. Am. Chem. Soc.,* **2008**, *130*, 6010-6017; g) D. N. Dybtsev; H. Chun, K. Kim. *Angew. Chem. Int. Ed.,* **2004**, *43*, 5033-5036; h) P. K. Thallapally; J. Tian; M. Radha Kishan; C. A. Fernandez; S. J. Dalgarno; P. B. McGrail; J. E. Warren, J. L. Atwood. *J. Am. Chem. Soc.,* **2008**, *130*, 16842-16843.

[4] a) S. Yuan; L. Zou; H. Li; Y. P. Chen; J. Qin; Q. Zhang; W. Lu; M. B. Hall, H. C. Zhou. *Angew. Chem. Int. Ed.,* **2016**, *55*, 10776-10780; b) J. Su; S. Yuan; H.-Y. Wang; L. Huang; J.-Y. Ge; E. Joseph; J. Qin; T. Cagin; J.-L. Zuo, H.-C. Zhou. *Nat. Comm.,* **2017**, *8*, 2008; c) A.-X. Zhu; Q.-Y. Yang; A. Kumar; C. Crowley; S. Mukherjee; K.-J. Chen; S.-Q. Wang; D. O′ Nolan; M. Shivanna, M. J. Zaworotko. *J. Am. Chem. Soc.,* **2018**, *140*, 15572-15576; d) M. Shivanna; Q.-Y. Yang; A. Bajpai; S. Sen; N. Hosono; S. Kusaka; T. Pham; K. A. Forrest; B. Space; S. Kitagawa, M. J. Zaworotko. *Science Advances,* **2018**, *4*, eaaq1636; e) J. Rabone; Y.-F. Yue; S. Y. Chong; K. C. Stylianou; J. Bacsa; D. Bradshaw; G. R. Darling; N. G. Berry; Y. Z. Khimyak; A. Y. Ganin; P. Wiper; J. B. Claridge, M. J. Rosseinsky. *Science,* **2010**, *329*, 1053-1057.

[5] a) S. Bourrelly; P. L. Llewellyn; C. Serre; F. Millange; T. Loiseau, G. Férey. *J. Am. Chem. Soc.,* **2005**, *127*, 13519-13521; b) S. Couck; J. F. M. Denayer; G. V. Baron; T. Rémy; J. Gascon, F. Kapteijn. *J. Am. Chem. Soc.,* **2009**, *131*, 6326-6327; c) V. Bon; N. Klein; I. Senkovska; A. Heerwig; J. Getzschmann; D. Wallacher; I. Zizak; M. Brzhezinskaya; U. Mueller, S. Kaskel. *Phys. Chem. Chem. Phys.,* **2015**, *17*, 17471-17479; d) F. Salles; G. Maurin; C. Serre; P. L. Llewellyn; C. Knöfel; H. J. Choi; Y. Filinchuk; L. Oliviero; A. Vimont; J. R. Long, G. Férey. *J. Am. Chem. Soc.,* **2010**, *132*, 13782-13788; e) B. Mu; F. Li; Y. Huang, K. S. Walton. *J. Mater. Chem.,* **2012**, *22*, 10172-10178; f) S. Henke; A. Schneemann; A. Wütscher, R. A. Fischer. *J. Am. Chem. Soc.,* **2012**, *134*, 9464-9474.

[6] a) F.-X. Coudert; C. Mellot-Draznieks; A. H. Fuchs, A. Boutin. *J. Am. Chem. Soc.,* **2009**, *131*, 11329-11331; b) D. Fairen-Jimenez; S. A. Moggach; M. T. Wharmby; P. A. Wright; S. Parsons, T. Düren. *J. Am. Chem. Soc.,* **2011**, *133*, 8900-8902; c) J.-J. Zheng; S. Kusaka; R. Matsuda; S. Kitagawa, S. Sakaki. *J. Am. Chem. Soc.,* **2018**, *140*, 13958-13969; d) Q. Yang; D. Liu; C. Zhong, J.-R. Li. *Chem. Rev.,* **2013**, *113*, 8261-8323.

[7] a) H.-S. Choi, M. P. Suh. *Angew. Chem. Int. Ed.,* **2009**, *48*, 6865-6869; b) S.-m. Hyun; J. H. Lee; G. Y. Jung; Y. K. Kim; T. K. Kim; S. Jeoung; S. K. Kwak; D. Moon, H. R. Moon. *Inorg. Chem.,* **2016**, *55*, 1920-1925.

[8] a) N. Nijem; H. Wu; P. Canepa; A. Marti; K. J. Balkus; T. Thonhauser; J. Li, Y. J. Chabal. *J. Am. Chem. Soc.,* **2012**, *134*, 15201-15204; b) L. Li; R. Krishna; Y. Wang; J. Yang; X. Wang, J. Li. *J. Mater. Chem. A,* **2016**, *4*, 751-755; c) M. L. Foo; R. Matsuda; Y. Hijikata; R. Krishna; H. Sato; S. Horike; A. Hori; J. Duan; Y. Sato; Y. Kubota; M. Takata, S. Kitagawa. *J. Am. Chem. Soc.,* **2016**, *138*, 3022-3030.

[9] a) S. Yang; X. Lin; W. Lewis; M. Suyetin; E. Bichoutskaia; J. E. Parker; C. C. Tang; D. R. Allan; P. J. Rizkallah; P. Hubberstey; N. R. Champness; K. Mark Thomas; A. J. Blake, M. Schröder. *Nat. Mater.,* **2012**, *11*, 710; b) E. R. Engel; A. Jouaiti; C. X. Bezuidenhout; M. W. Hosseini, L. J. Barbour. *Angew. Chem. Int. Ed.,* **2017**, *56*, 8874-8878.

[10] Y. Sakata; S. Furukawa; M. Kondo; K. Hirai; N. Horike; Y. Takashima; H. Uehara; N. Louvain; M. Meilikhov; T. Tsuruoka; S. Isoda; W. Kosaka; O. Sakata, S. Kitagawa. *Science,* **2013**, *339*, 193-196.

[11] a) M. Behl; M. Y. Razzaq, A. Lendlein. *Adv. Mater.,* **2010**, *22*, 3388-3410; b) R. Kainuma; Y. Imano; W. Ito; Y. Sutou; H. Morito; S. Okamoto; O. Kitakami; K. Oikawa; A. Fujita; T. Kanomata, K. Ishida. *Nature,* **2006**, *439*, 957-960.

[12] a) M. Shivanna; Q.-Y. Yang; A. Bajpai; S. Sen; N. Hosono; S. Kusaka; T. Pham; K. A. Forrest; B. Space; S. Kitagawa, M. J. Zaworotko. *Sci. Adv.,* **2018**, *4*, 1636; b) M. Shivanna; Q.-Y. Yang; A. Bajpai; E. Patyk-Kazmierczak, M. J. Zaworotko. *Nat. Comm.,* **2018**, *9*, 3080.

[13] a) Q.-G. Zhai; X. Bu; C. Mao; X. Zhao; L. Daemen; Y. Cheng; A. J. Ramirez-Cuesta, P. Feng. *Nat. Comm.,* **2016**, *7*, 13645; b) Q.-G. Zhai; X. Bu; X. Zhao; C. Mao; F. Bu; X. Chen, P. Feng. *Cryst. Growth Des.,* **2016**, *16*, 1261-1267; c) X.-J. Lei; X.-Y. Hou; S.-N. Li; Y.-C. Jiang; G.-X. Sun; M.-C. Hu, Q.-G. Zhai. *Inorg. Chem.,* **2018**, *57*, 14280-14289; d) P. Ramaswamy; N. E. Wong; B. S. Gelfand, G. K. Shimizu. *J. Am. Chem. Soc.,* **2015**, *137*, 7640-7643.

[14] P. Horcajada; F. Salles; S. Wuttke; T. Devic; D. Heurtaux; G. Maurin; A. Vimont; M. Daturi; O. David; E. Magnier; N. Stock; Y. Filinchuk; D. Popov; C. Riekel; G. Férey, C. Serre. *J. Am. Chem. Soc.,* **2011**, *133*, 17839-17847.

[15] a) F. Rouquerol; J. Rouquerol, K. Sing. *Adsorption by powders and porous solids. Academic Press, London.,* **1999**, 204-206; b) A. Gil; S. A. Korili, M. A. Vicente. *Catal. Rev. Sci. Eng.,* **2008**, *50*, 153-221.

[16] X. Li; X. Chen; F. Jiang; L. Chen; S. Lu; Q. Chen; M. Wu; D. Yuan, M. Hong. *Chem. Commun.,* **2016**, *52*, 2277-2280.

[17] J. Ma; A. P. Kalenak; A. G. Wong-Foy, A. J. Matzger. *Angew. Chem. Int. Ed.,* **2017**, *56*, 14618-14621.

[18] L. Chen; J. P. Mowat; D. Fairen-Jimenez; C. A. Morrison; S. P. Thompson; P. A. Wright, T. Düren. *J. Am. Chem. Soc.,* **2013**, *135*, 15763-15773.

[19] a) H. J. Choi; M. Dincă, J. R. Long. *J. Am. Chem. Soc.,* **2008**, *130*, 7848-7850; b) M. K. Taylor; T. Runčevski; J. Oktawiec; M. I. Gonzalez; R. L. Siegelman; J. A. Mason; J. Ye; C. M. Brown, J. R. Long. *J. Am. Chem. Soc.,* **2016**, *138*, 15019-15026.

[20] E. J. Carrington; C. A. McAnally; A. J. Fletcher; S. P. Thompson; M. Warren, L. Brammer. *Nat. Chem.,* **2017**, *9*, 882.

[21] K.-J. Chen; Hayley S. Scott; David G. Madden; T. Pham; A. Kumar; A. Bajpai; M. Lusi; Katherine A. Forrest; B. Space; John J. Perry, Michael J. Zaworotko. *Chem,* **2016**, *1*, 753-765.

[22] a) R.-B. Lin; L. Li; H. Wu; H. Arman; B. Li; R.-G. Lin; W. Zhou, B. Chen. *J. Am. Chem. Soc.,* **2017**, *139*, 8022-8028; b) P. Li; Y. He; Y. Zhao; L. Weng; H. Wang; R. Krishna; H. Wu; W. Zhou; M. O'Keeffe; Y. Han, B. Chen. *Angew. Chem. Int. Ed.,* **2015**, *54*, 574-577.

[23] Y. Ye; Z. Ma; R.-B. Lin; R. Krishna; W. Zhou; Q. Lin; Z. Zhang; S. Xiang, B. Chen. *J. Am. Chem. Soc.,* **2019**, *141*, 4130-4136.

Entry for the Table of Contents (Please choose one layout)

COMMUNICATION

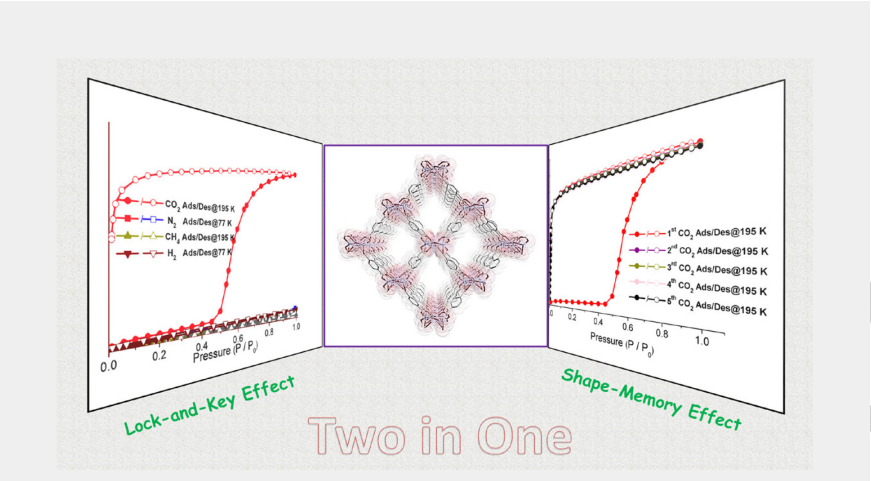

A chilling pore opening: a cold CO_2 stream becomes the secret code for opening a tightly sealed and extra-framework-cation-guarded anionic Mg-MOF. Once open, various gas molecules can freely dance into or swing out of rigidized channels, until being locked out again.

Huajun Yang, Thuong Xinh Trieu, Xiang Zhao, Yanxiang Wang, Yong Wang, Pingyun Feng, and Xianhui Bu**

Page No. – Page No.

Lock-and-Key and Shape-Memory Effects in an Unconventional Synthetic Path to Magnesium-Organic Frameworks